ChemPlusChem

Research Article
doi.org/10.1002/cplu.202300743

Chemistry Europe
European Chemical Societies Publishing

www.chempluschem.org

Amphiphilic Chlorin-β-cyclodextrin Conjugates in Photo-Triggered Drug Delivery: The Role of Aggregation

Stylianos Panagiotakis,[a] Barbara Mavroidi,[b] Alexandros Athanasopoulos,[b] Georgios Charalambidis,[c, d] Athanassios G. Coutsolelos,[c] Maria Pelecanou,[b] and Konstantina Yannakopoulou*[a]

Conjugates of chlorins with β-cyclodextrin connected either directly or via a flexible linker were prepared. In aqueous medium these amphiphilic conjugates were photostable, produced singlet oxygen at a rate similar to clinically used temoporfin and formed irregular nanoparticles via aggregation. Successful loading with the chemotherapeutic drug tamoxifen was evidenced in solution by the UV-Vis spectral changes and dynamic light scattering profiles. Incubation of MCF-7 cells with the conjugates revealed intense spotted intracellular fluorescence suggestive of accumulation in endosome/lysosome compartments, and no dark toxicity. Incubation with the tamoxifen-loaded conjugates revealed also practically no dark toxicity. Irradiation of cells incubated with empty conjugates at 640 nm and 4.18 J/cm^2 light fluence caused $>50\%$ cell viability reduction. Irradiation following incubation with tamoxifen-loaded conjugates resulted in even higher toxicity (74%) indicating that the produced reactive oxygen species had triggered tamoxifen release in a photochemical internalization (PCI) mechanism. The chlorin-β-cyclodextrin conjugates displayed less-lasting effects with time, compared to the corresponding porphyrin-β-cyclodextrin conjugates, possibly due to lower tamoxifen loading of their aggregates and/or their less effective lodging in the cell compartments' membranes. The results suggest that further to favorable photophysical properties, other parameters are important for the *in vitro* effectiveness of the photodynamic systems.

Introduction

Cyclodextrins (CDs) are cyclic water-soluble glucopyranose oligomers, well-established as molecular carriers of hydrophobic molecules, in particular insoluble drugs. The carrier properties of CDs stem from their hollow structure that defines an inner hydrophobic space where the guest molecules are hosted. The outer surface is decorated with numerous hydroxyl groups that confer solubility in water.[1] The interest in CDs is continuously renewed due to the emergence of new drug delivery opportunities.[2]

Porphyrinoids are molecules that can act as photo-sensitizers (PSs) in photodynamic therapy (PDT), owing to their suitable photophysical properties. Specifically, upon light irradiation in the red to the far-red region of the spectrum (600–800 nm) and in the presence of molecular oxygen, the PSs produce reactive oxygen species (ROS), most importantly singlet oxygen ($^1O_2$). This results in efficient photokilling of cancerous cells in the tissue where the PS is accumulated. Several PSs have found their way to the clinic for PDT treatment of malignancies.[3]

Photochemical Internalization (PCI) is an advanced modality where a chemotoxic drug is endocytosed and accumulated in endosomes and lysosomes, while the administered PS is embedded in the membranes of these compartments. Suitable irradiation activates the production of reactive oxygen species (ROS), such $^1O_2$, that damage the membranes causing release of the drug in the cytosol where it can exert its toxic effect. PCI has been introduced as a method to deliver macromolecular drugs in the cells.[4] Notably, both PDT and PCI confer vascular damage as well as immune responses that contribute to tumor cell death.[3b,4c]

By covalently linking CDs with porphyrinoids, conjugates with dual capacity, i.e., drug delivery and ROS photoproduction, are obtained. Some covalent porphyrin-CD conjugates have been reported to be effective agents under PDT conditions, mostly in *in vitro* experiments under varying incubation and irradiation protocols and in combination with different anticancer drugs.[5] The utility and promise of porphyrin-CD

[a] Dr. S. Panagiotakis, Dr. K. Yannakopoulou
Institute of Nanoscience and Nanotechnology
National Center for Scientific Research "Demokritos"
Patr. Grigoriou E' & 27 Neapoleos str., 15341 Aghia Paraskevi, Attiki, Greece
E-mail: k.yannakopoulou@inn.demokritos.gr

[b] Dr. B. Mavroidi, Dr. A. Athanasopoulos, Dr. M. Pelecanou
Institute of Biosciences & Applications
National Center for Scientific Research "Demokritos"
Patr. Grigoriou E' & 27 Neapoleos str., 15341 Aghia Paraskevi, Attiki, Greece

[c] Dr. G. Charalambidis, Prof. Dr. A. G. Coutsolelos
Laboratory of Bioinorganic Chemistry
Department of Chemistry
University of Crete
Voutes Campus, 70013 Heraklion, Crete, Greece

[d] Dr. G. Charalambidis
Charalambidis' current address:
Theoretical and Physical Chemistry Institute
National Hellenic Research Foundation
48 Vas. Constantinou Ave., 11635 Athens, Greece

Supporting information for this article is available on the WWW under https://doi.org/10.1002/cplu.202300743

conjugates for applications in PCI protocols and delivery of small anticancer drugs have been initially highlighted using a *meso*-(m-hydroxypheny)porphyrin-β-CD (mTHPP-βCD) conjugate[6] that enabled the delivery of small chemotherapeutics, and recently consolidated with several strongly amphiphilic *meso*-tetraphenylporphyrin-βCD (TPP-βCD) conjugates.[7] These conjugates self-assembled to stable ~60 nm nanoparticles (NPs) that could be loaded with anticancer drugs *via* both cavity inclusion and entanglement in the NP formation. The drug-loaded NPs selectively accumulated in the endocytic vesicles of breast adenocarcinoma MCF-7 cells, displayed no dark toxicity, whereas, following suitable irradiation, they conferred significant reduction of cell viability (>85%), exhibiting highly synergistic 24 h photo- and chemo-toxicity that was sustained for 48 h, suggesting a PCI mechanism of drug release.

Chlorins, obtained from porphyrins by the reduction of one pyrrole double bond, absorb light more efficiently in the therapeutic window of the body (650 to 700 nm)[3b] than porphyrins. Several chlorins have been approved for clinical use.[3b,8–10] Temoporfin (*meso*-(m-hydroxypheny)chlorin, mTHPC)[10b] has been approved by the EMA for the treatment of advanced head and neck cancer (Foscan®). Literature on chlorin-CD conjugates is scarce: a water-soluble pentafluorophenyl- chlorin connected to four βCD units was an effective PS in PDT treatment of human keratinocytes.[11] Further, a chlorin e6-βCD-folic acid conjugate targeting HeLa cells upon irradiation displayed higher reduction of cell viability than chlorin e6 alone and also resulted in considerable inhibition of tumor growth of HeLa-derived xenografts on mice.[12]

The present work aims to investigate the effectiveness of chlorin-βCD conjugates in photo-controlled delivery of the small anticancer drug tamoxifen citrate (TamCit), a non-steroidal selective estrogen receptor modulator (SERM) that is suitable for treating the estrogen receptor-positive MCF-7 cells. To this end, the conjugate mTHPCCD where mTHPC is directly connected to one primary OH group of βCD, and the non-hydroxylated, highly amphiphilic conjugate TPCOCNHbmC5 where tetraphenylchlorin (TPC) is connected to βCD *via* a C5-aliphatic linker (Scheme 1a) were prepared, studied and their PCI performance was evaluated. The results were compared with the performance of the corresponding porphyrin conjugates, mTHPPCD and TPPOCNHbmC5, under identical experimental conditions,[7] aiming to highlight the factors that influence their effectiveness *in vitro*.

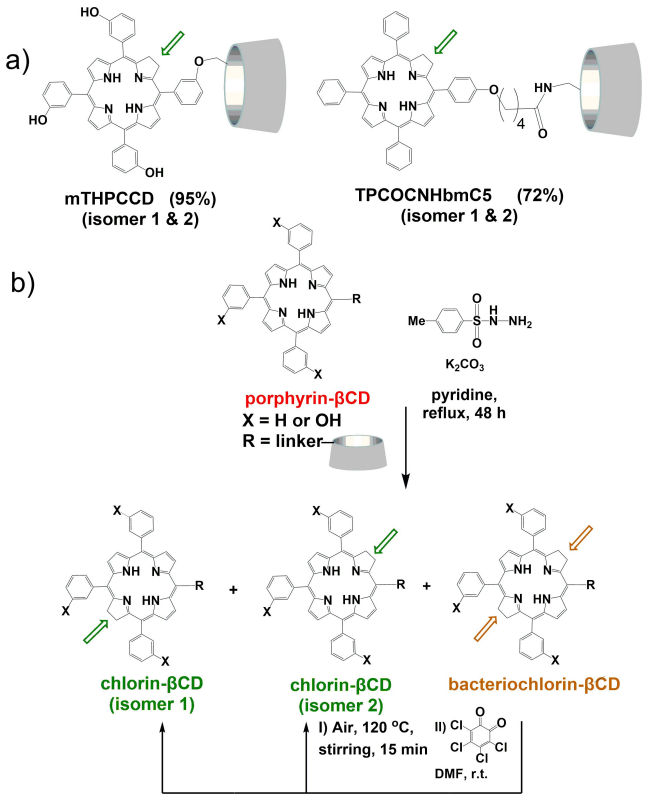

Scheme 1. a) The chlorin-βCD conjugates; b) their synthesis.

Results and Discussion

Synthesis

The most convenient method to prepare chlorin-βCD conjugates is the selective reduction of a single pyrrole ring of porphyrin-βCD conjugates. Previously synthesized mTHPPCD[6] and TPPOCNHbmC5[7] were treated according to the Whitlock diimide procedure[13] (Scheme 1b), adopted from the literature[14] with modifications. The reaction progress was assessed by monitoring the disappearance of the porphyrin Q band at 646 nm and the emergence of the chlorin Q band at 650 nm in the UV-Vis spectrum of the reaction mixture. The reaction progress was additionally monitored with ^{1}H NMR spectra focusing on the endocyclic NH signals.

The products were obtained in good yields as inseparable mixtures of isomers having the dihydropyrrole ring either adjacent or opposite to the βCD-substituted phenyl ring (isomer 1 and isomer 2, Scheme 1b), as previously observed for gluco-conjugated chlorins.[14] In case of over-reduction to undesired bacteriochlorin-βCD (Scheme 1b) evidenced by a Q band at 740 nm, oxidation to chlorin-βCD was induced by tetrachloro-*o*-benzoquinone (*o*-chloranil). Formation of isobacteriochlorin-βCD (two adjacent dihydropyrrole rings) was considered unfavorable. The clinically used mTHPC was also prepared from the corresponding porphyrin mTHPP, for comparison.

Structural Characterization

The chlorin-βCD conjugates displayed complex ^{1}H NMR spectra in DMSO-d_6, mainly in the aromatic region, presumably due to the presence of the two isomers. With the help of 2D NMR spectra, assignment of the majority of the signals was accomplished (Figures S1-S4). Integration of the endocyclic NH signals and selected βCD signals in the ^{1}H NMR spectra confirmed the 1:1 conjugation. Two NH signals were observed at −1.63 ppm and −1.65 ppm for mTHPCCD and at −1.53 ppm and −1.58 ppm for TPCOCNHbmC5 (Figure S5) indicative of

slowly exchanging tautomers influenced by the presence of the βCD substituent.[15] Integration of the two NH signals in each sample provided a nearly 1:1 ratio while noticeable broadness was also displayed, particularly for the most shielded signal, as also reported for the TPC-chitosan conjugates.[14,16] For TPCOCNHbmC5 and mTHPCCD samples, a weak NH signal at −2.90 ppm revealed residues of the starting porphyrin-βCDs, determined by integration as <4% and <10%, respectively, which were impossible to either completely reduce[13b] or remove by chromatography. A single molecular ion/base peak was registered in each positive mode MALDI-ToF mass spectrum (Figures S6, S7) while the similar FT-IR spectra of the samples displayed the expected bands of the chlorin and βCD moieties and the amide band of TPCOCNHbmC5 at 1647 cm^{-1} (Figure S8).

Absorption, Emission and Emission Decay Spectra

The UV-Vis spectra in DMF (Figure 1a) were typical of free-base *meso*-substituted chlorins[17] with one B band (Soret) in the region 375–450 nm and four Q bands in the region 500–675 nm. Whereas the extinction coefficient (ε) values of the Soret band of the chlorin-βCD conjugates (Table 1) were 3-fold lower, compared to the corresponding porphyrin-βCD conjugates,[7] the ε values of the Q(0,0) bands (651.5 nm) were 4 or 5-fold higher. This feature suggests that the chlorin-βCD conjugates could be more efficient as red-light harvesting units. Second derivative analysis of the UV-Vis spectra (Figure S9 inset and Table S1) assisted in understanding the effects.

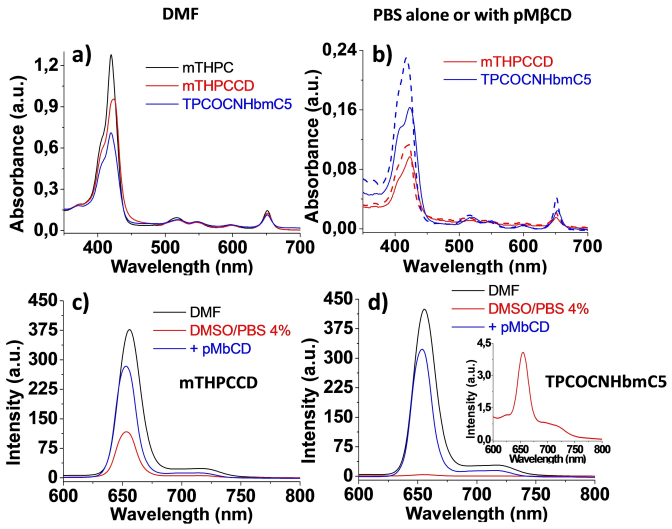

Figure 1. (a, b): Absorption spectra of mTHPCCD (6 μM), and TPCOCNHbmC5 (6 μM) in a) DMF (the starting mTHPC, 6 μM, is included) and b) PBS with 4% DMSO, v/v, alone (solid lines) and as complexes with 2,3,6-tri-*O*-methyl-β-cyclodextrin (pMβCD, dotted lines); (c,d): Emission spectra (λ_{ex} = 517 nm) in DMF and PBS with 4% DMSO, v/v of c) mTHPCCD (6 μM) and d) TPCOCNHbmC5 (6 μM); inset is the magnified spectrum.

In contrast to DMF solution, in phosphate buffer saline (PBS, pH 7.4) with 4% DMSO (v/v) solution the absorption spectra of mTHPCCD exhibited significant hypochromicity, broadening and very slightly blue-shifted Soret and Q bands, whereas the spectra of TPCOCNHbmC5 displayed measurable red shifts of the absorption bands (Figure 1b, solid lines, Table 1). The spectrum of unconjugated mTHPC in PBS displayed not only clear broadening but also red shift (7 nm) of the major band signifying aggregation[18a] most likely of the J-type.[18b] Conjugation to βCD yielded two isomers for each case[18c] and two bands of unequal intensity near 419 and 427 nm in the spectra in DMF (Figure S9, insets, blue lines and Table S1). In PBS the two conjugates behaved differently (Figure S9, insets, black lines and Table S1): the spectrum of mTHPCCD showed one strong broad band at 422 nm, which could be partially attributed to aggregation *via* self-inclusion of the chlorin moiety inside another βCD cavity; the spectrum of TPCOCNHbmC5 with two strong broad peaks at 405 nm and 426 nm could indicate formation of both H- and J-aggregates.[18] In this case, the C5 linker that separates sufficiently the chlorin and βCD moieties presumably allows aggregation of the chlorin part by different stacking modes.

It is established that 2,3,6-tri-*O*-methyl-β-cyclodextrin (pMβCD) forms strong 2:1 complexes with *meso*-arylporphyrins,[19] porphyrin-βCD conjugates,[7] and mTHPC.[20] Addition of pMβCD in the solutions of the chlorin-βCD conjugates resulted in enhanced absorption intensity, most spectacular for TPCOCNHbmC5, and blue-shifted Soret bands (Figure 1b, dashed lines). Best fit of the UV-Vis titration data with pMβCD (Figure S10) confirmed very strong complexation with either 1:1 (pMβCD/mTHPCCD, $K = 25.76\times10^6$ M^{-1}), or 2:1 (pMβCD/TPCOCNHbmC5, $K = 8.23\times10^9$ M^{-2}) stoichiometries (Table S2). Evidently, inclusion of the chlorin moiety by pMβCD from two opposite sides in TPCOCNHbmC5 decreased considerably the aggregation, while one side inclusion in mTHPCCD was less effective, maybe due to the presence of stable, self-included aggregates.

The emission properties of the conjugates in DMF were characteristic of free-base chlorins[17] with two emission bands between 600 and 800 nm (Figures 1c,d, black lines). The

Table 1. Absorption and emission data[a] of chlorin-βCD conjugates (isomer 1 and isomer 2) in different solvents and after complexation with pMβCD.

Chlorins	λ_{max} (ε)[b] DMF	λ_{em} (Φ)[c], DMF	λ_{max} Aq[d]	λ_{em} Aq[d,e]	λ_{max} Aq[d] + pMβCD	λ_{em} Aq[d,e] + pMβCD
mTHPC	420.0 (213.2) 651.5 (24.2)	656, 716 (0.172)	–	–		
mTHPC-CD	423.5 (159.4), 651.5 (21.0)	656, 716 (0.159)	423.0, 651.0	653, 715	422.0, 650.5	653, 714
TPCOC-NHbmC5	419.5 (118.5), 651.5 (19.0)	656, 715 (0.181)	422.5, 652.5	655, 714	417.5, 651.0	654, 713

[a] λ_{max} and λ_{em} in nm; [b] extinction coefficient, ε/10^3 $M^{-1}cm^{-1}$; [c] Φ = quantum yield; [d] Aq = PBS with 4% DMSO (v/v); [e] λ_{ex} = 517 nm, corresponding to the respective Q(1,0) bands.

fluorescence quantum yield (Φ) values were very similar to those of mTHPC (Table 1).

In the aqueous medium the emission of mTHPCCD was sufficiently sustained (Figure 1c, red line) whereas the emission of the strongly amphiphilic TPCOCNHbmC5 (Figure 1d, red line) was substantially quenched. Differences in the linkers between chlorin and βCD moieties and presence or absence of OH groups in the chlorin structure (Scheme 1a) clearly impact the emission properties. The weak fluorescence of TPCOCNHbmC5 can be attributed to emission-quenching H-aggregates and the fact that J-aggregates have low fluorescence quantum yields.[18b] Addition of pMβCD (Figure 1c, d, blue lines) resulted in dramatically increased fluorescence intensities, particularly for TPCOCNHbmC5, providing further evidence for inclusion complexation-mediated de-aggregation and improved solubility, in agreement with the UV-Vis spectroscopic results.

Best fits of the emission decay spectra in DMF and in PBS pH 7.4 with 4% DMSO (v/v), (Figure S11) using mono- or biexponential functions, yielded the lifetime (τ) values (Table 2). In the presumed monomerizing solvent DMF[21] the single τ value indicated the presence of a single emitting species for all compounds. In the aqueous medium the single 10.3 ns lifetime of mTHPCCD was slightly higher than the lifetime of the parent mTHPPCD (9.4 ns, 74%).[22] The predominant photoactive species in mTHPCCD could be the self-included complex that contributes to preserving the photophysical profile of the mTHPC moiety with considerable fluorescence (Figure 1c, red line). The two τ values of TPCOCNHbmC5 due to a faster-decaying species ($\tau1 = 0.4$ ns, 47%) and a longer-lived species ($\tau2 = 5.2$ ns, 53%) (Table 2), could arise from the J- and H-aggregates.[18] pMβCD restored the lifetimes, especially of TPCOCNHbmC5, due to effective monomerization of the chlorin moieties.

Dynamic Light Scattering (DLS)

DLS measurements of the chlorin- βCD conjugates (2 μM) were performed in PBS with 4% DMSO (v/v) (Table S3) in order to compare the DLS results with those of the porphyrin precursors using the same concentrations in the same solvent and taking into account the limitations of measuring colored samples. In the measurements of the mTHPCCD sample (Figure S12A,B), despite the good signal-to-noise ratio indicated by the high intercept value of the correlation function (~90%, Figure S12C), the large variability of the size distribution by intensity in the consecutive measurements (Figure S12A) indicated particle instability and rather random aggregation. The smaller variability and noticeable increase of the signal in the consecutive size distribution measurements for the TPCOCNHbmC5 sample (Figure S13A,B) could be attributed to further aggregation of the particles. Moreover, the low intercept of the correlation function with the Y-axis (~50%) indicated worst signal-to-noise ratio than in the mTHPCCD data. As both samples were measured using a 173° detector angle and a 633 nm laser where both compounds absorb very similarly and, moreover, mTHPCCD fluoresces much more intensely than TPCOCNHbmC5 in PBS with 4% DMSO (v/v), it is not reasonable to attribute the low DLS signal of TPCOCNHbmC5 to multiple scattering effects or to fluorescence-generated noise. Some sedimentation could be responsible for the moderate TPCOCNHbmC5 signals. Furthermore, in all measurements the distribution fits were rather unsatisfactory: relatively large Polydispersity Index (PDI) values were calculated, co-presence of large particles was indicated and the correlograms did not overplot (Figures S12, S13 C,D), suggesting unstable aggregates, for which zeta potential values could not be obtained. The considerable departure from the spherical shape of the particles and the fact that two isomers coexist in each product which probably assemble differently, could contribute to the unsatisfactory quality of the data. At concentrations >2 μM the variability of the data and the calculated PDI values became even higher. Comparison of the TPCOCNHbmC5 and TPPOCNHbmC5 DLS data (Table S3) suggests that the single dihydropyrrole ring in the chlorin moieties compels the conjugates to organize in larger, irregular aggregates quite differently than the parent porphyrin conjugates that form relatively uniform ~60 nm NPs.

Complexation with Tamoxifen

In the presence of the anticancer drug tamoxifen citrate (TamCit) which forms relatively strong complexes with βCD (~7×10^3 M^{-1}),[23] the DLS data of both conjugates displayed a noticeable quality improvement with stronger signals, better correlation diagrams (Figures 2A, B Figures S14, S15), smaller-sized particles and somewhat improved PDI (Table S3), suggesting better organization of the aggregates due to guest-promoted aggregation[24] and improved NP formation. In contrast, incubation of the parent porphyrin conjugate mTHPPCD with TamCit caused increase of the ~80 nm NPs to various undetermined sizes (Table S3) indicating that immediate

Table 2. Emission lifetime (τ) data of chlorin-βCD conjugates (6 mM) in different solvents and after addition of pMβCD.

Chlorins	τ (ns) DMF	τ (ns) 4% Aq[b]		τ (ns) 4% Aq[b] + pMβCD	
		$\tau1$	$\tau2$	$\tau1$	$\tau2$
mTHPC	9.4[a]	–	–	–	–
mTHPCCD	8.9[a]	10.3[a]	–	10.7[a]	–
TPCOCNHbmC5	9.3[a]	0.4[c]	5.2[d]	11.9[a]	–

Values ±0.1 ns; [a] 100%; [b] Aq = PBS, with 4% DMSO (v/v); [c] 47%; [d] 53%.

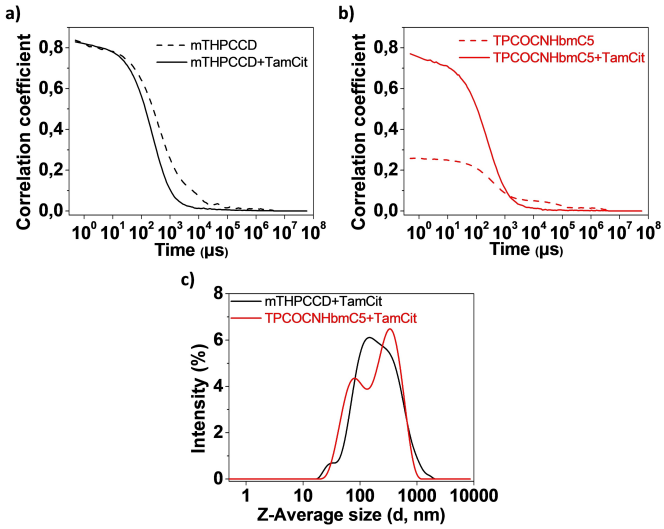

Figure 2. DLS measurements of the chlorin-βCD conjugates (2 μM in PBS with 4% DMSO v/v): diagrams of a,b) distribution fit for the conjugate alone (–·–) and in the presence of tamoxifen citrate (TamCit) (–––) and c) size distribution by intensity of the conjugates after incubation with TamCit.

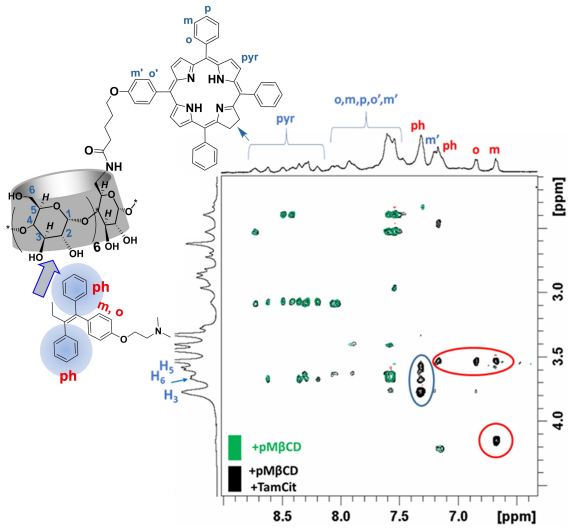

Figure 3. Partial 2D ROESY spectrum (500 MHz, 298 K, PBS with 4% DMSO, v/v) of the complex pMβCD/TPCOCNHbmC5 (1.53 mM : 1.70 mM) in the presence of TamCit (1.12 mM) (black cross-peaks), overlaid with the 2D ROESY spectrum of the complex pMβCD/TPCOCNHbmC5 (1.53 mM : 1.70 mM) (green cross-peaks). Blue ellipse: intermolecular interactions between TamCit and TPCOCNHbmC5 cavity protons. Red circle/ellipse: intramolecular interactions within the TamCit structure.

attachment of mTHPP onto βCD (Scheme 1a) tolerates only fragile organization of the aggregates which crumble upon entrance of TamCit in the cavity. In comparison, the ~60 nm NPs of TPPOCNHbmC5 expand to larger but still functional ~120 nm NPs[7] due to both inclusion in βCD and incorporation of TamCit in the NPs structure.

^{1}H NMR spectra were obtained with the help of pMβCD which sustained the conjugates in the aqueous solution at mM concentrations. Highly shielded signals of pMβCD due to inclusion complexation of the chlorin moiety of the conjugates were observed (TPCOCNHbmC5 Figure 3; mTHPCCD Figure S16). Slow exchange between free and complexed pMβCD was observed, as with the parent porphyin-βCD conjugates.[7] The pattern and the frequencies of the signals were precisely the same in both conjugates and nearly the same as in the porphyrin precursors reported earlier,[7,19] denoting very similar inclusion complexation modes with pMβCD. Addition of TamCit resulted in the establishment of an additional complexation equilibrium in fast exchange because of the inclusion into the available βCD cavities. The signals of TamCit displayed clear through-space dipolar interactions with the chlorin-βCD cavity protons (H3, H5 and H6) (Figure 3, Figure S16, blue ellipse). The intensities of these cross-peaks were comparable with those of the intramolecular cross-peaks (red circle/ellipse), indicating quite strong inclusion complexation. Thus, the chlorin-βCD conjugates can host the drug in a similar fashion as the parent porphyrin-βCD conjugates.

Moreover, addition of TamCit in the aqueous solution of the conjugates resulted in red-shifted λ_{max} in the UV-Vis spectra, especially for TPCOCNHbmC5 (Figure S9, inset, red lines and Table S1). In contrast, addition of TamCit to a solution of the clinically used mTHPC did not result in any spectral changes, indicating that TamCit does not interact with mTHPC and that the βCD cavity plays a pivotal role in the drug loading of the aggregated conjugates. Being mixtures of isomers, each of which may assemble in a different manner, the conjugates become better organized in the presence of TamCit and their aggregates become smaller in size. Some entanglement of tamoxifen in the assemblies cannot be ruled out.

Cell Experiments

Irradiation of the conjugates in PBS with 4% DMSO at 630 ± 10 nm with a 0.741 W LED photoreactor for 60 min revealed good photostability, comparable to mTHPC: after an initial drop of the Soret band intensity (Figure S17), the photobleaching reached a plateau with 80% photoactivity preserved after 1 h, suggesting suitability of the conjugates for use in live cell imaging with confocal microscopy. Thus, MCF-7 human breast adenocarcinoma cells were incubated for 24 h with the pre-assembled conjugates and with mTHPC alone. The cell images with mTHPC showed intense diffuse red fluorescence distributed throughout the cytoplasm compartments (Figure 4a1, left), consistent with literature that reports endoplasmic reticulum (ER) as preferred for localization and accumulation of Foscan® in MCF-7 cells, after 24 h incubation.[25]

In contrast, the chlorin conjugates displayed intense spotted fluorescence (Figure 4a1 middle and right) indicative of endosomal/lysosomal accumulation, as also observed with the corresponding porphyrin conjugates.[7] Indeed, co-staining with LysoTracker® Green DND-26 confirmed satisfactory co-localization with the conjugates (Figure 4a2). The molecular size of the conjugates, their enhanced amphiphilicity and their aggregation plausibly suggest uptake by endocytosis. Interestingly, mTHPCCD and TPCOCNHbmC5 display qualitatively very

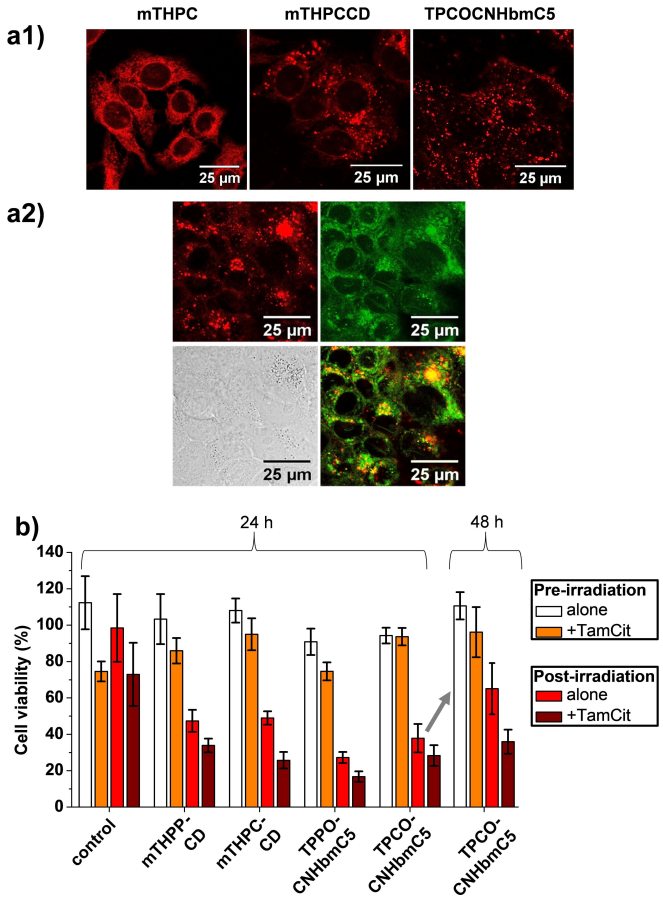

Figure 4. a) Confocal microscopy images (laser intensity: 3.0%) of MCF-7 cells following 24 h incubation with compounds (10 μM): a1) mTHPC, mTHPCCD and TPCOCNHbmC5, a2) TPCOCNHbmC5 (red fluorescence, top-left) and LysoTracker® Green DND-26 (green fluorescence, top-right); overlay of the images (bottom-right) and the bright field image (bottom-left). b) Viability of MCF-7 cells following 24 h incubation without and with the chlorin-βCD conjugates, the corresponding porphyrin-βCD conjugates (10 μM) either alone or loaded with TamCit (7.5 μM). Following irradiation (4.18 J/cm^2, 640 nm LED-array) the MTT assays were performed after 24 h. Cells treated with TPCOCNHbmC5 either alone or TamCit-loaded, were assayed 24 h and 48 h post-irradiation.

similar intracellular emission, despite the large difference in their fluorescence intensity in PBS solution (Figure 1C, D).

ROS generation with red light irradiation of the conjugates was tested in the presence of 9,10-anthracenediyl-bis(methylene)dimalonic acid (ABDA).[7,26] Singlet oxygen ($^1O_2$) production of the conjugates was registered at rates similar to the $^1O_2$ production of mTHPC (Figure S18, Table S4). Consequently, both conjugates were suitable for cell phototoxicity assessment. Untreated MCF-7 cells irradiated with increasing light doses (0→12.55 J/cm^2) using our irradiation setup (LED array lamp, 640 nm) did not suffer viability reduction (Figure 4b, control, 4.18 J/cm^2, red bar compared to white bar), as shown before.[7] Incubation of the cells for 24 h with TamCit alone resulted in ~25% reduction of viability without or with irradiation (control, orange bar compared to brown bar). Incubation of the cells with the pre-assembled empty conjugates mTHPCCD and TPCOCNHbmC5 and their porphyrin analogues, mTHPPCD and TPPOCNHbmC5[7], revealed absence of dark toxicity after 24 h (white bars). Additionally, incubation with the TamCit-loaded conjugates resulted practically in no viability reduction demonstrating satisfactory absence of dark toxicity (orange bars); actually, the viability of the cells was even higher than for TamCit alone (control, orange bar). The samples were subsequently irradiated at 640 nm at light-doses suitable to achieve LD50 or the highest synergistic effect (4.18 J/cm^2, Figure S19). As Figure 4b shows, the photodynamic (PDT) effect of all empty conjugates was significant, as cell viability dropped below 50% (red bars) after 24 h. The PDT effect of the chlorin-βCD conjugates was expected to be higher than the effect of the corresponding porphyrin-βCD conjugates owing to the higher absorption of the chlorin moiety in the red region (Q bands); however, porphyrin TPPOCNHbmC5 displayed the highest phototoxicity, conferring ~73% reduction of viability whereas TPCOCNHbmC5 (61%), mTHPPCD (55%), and mTHPCCD (51%) were less effective. Irradiation of TamCit-loaded conjugates resulted clearly in further decrease of cell viability (brown bars): TPPOCNHbmC5 (83%), TPCOCNHbmC5 (72%) mTHPCCD (74%), and mTHPPCD (66%). Given that the TamCit-loaded conjugates had no dark toxicity, it can be assumed that red-light illumination resulted in release of the confined TamCit from the vesicles allowing it to exert its cytotoxic action. Therefore, a PCI mechanism can be suggested to explain the results. MTT assay 48 h post irradiation (Figure 4b, last set) of cells treated with TPCOCNHbmC5 alone showed cell recovery with only 35% viability reduction whereas cells treated with TamCit-loaded TPCOCNHbmC5 showed smaller recovery (~65% reduction), however the tendency for cell growth was evident.

Interaction of the amphiphilic chlorin-βCD aggregates with cell membrane components is expected to destabilize the aggregates but even complete dismantling would yield monomers that are too large (~2 kDa) to pass through the cell membranes. Therefore, endocytosis and entrapment in endosomes/lysosomes is anticipated in any case. Our previous studies showed[7] that solutions of porphyrin-βCD NPs incubated with model liposomes display identical UV-Vis spectra both in aqueous media and in the monomerizing solvent DMF, suggesting that the conjugates embed in the liposome membranes as monomers. This occurs without disturbing the liposome size and PDI values. We argued[7] that in a similar fashion the porphyrin-βCDs end up in the membranes of endosome/lysosome compartments and act as PSs upon irradiation compromising the membranes and releasing the drug. A similar mechanism is anticipated for the present chlorin-βCDs. Further, the fact that upon irradiation TamCit alone confers little damage to the cells but the TamCit/chlorin-βCD formulation becomes highly toxic, indicates that the whole system remains confined for 24 h until its activation by light.

The MCF-7 cell experiments indicate that although the chlorin-βCD conjugates display both PDT and PCI effects, they are rather less appropriate for PCI protocols than the corresponding porphyrins, which under the same conditions succeeded in suppressing efficiently cell growth 48 h post-irradiation.[7] Insufficient drug loading of the irregular aggregates, immediate drug release and/or less effective lodging of

the chlorin conjugates in the vesicle membranes could result in the observed less effective PCI *in vitro*.

Conclusions

The successful preparation of chlorin-βCD conjugates as photoactive drug carriers has been described. The conjugates form rather irregular aggregates which are improved in the presence of the chemotherapeutic drug tamoxifen citrate, presumably due to cavity inclusion. The conjugates are effectively taken up by MCF-7 cancer cells and reside into endosomes/lysosomes. The conjugates either alone or drug-loaded display negligible dark toxicity. Irradiation of the cells incubated with the conjugates alone results in moderate PDT effects (~50 to 60% cell viability 24 h post-irradiation). The effects are up to ~20% improved after irradiation of cells incubated with the drug-loaded conjugates, suggesting tamoxifen photo-release and operation of a PCI mechanism. The cells treated with TPCOCNHbmC5/TamCit seem to recover in the following 24 h, indicating that this system is less efficient than the porphyrin analogue, TPPOCNHbmC5/TamCit. The results suggest that the efficient formation of suitably-sized, stable, photoactive NPs with high drug payload seems to be more important than the absorption properties of the light-harvesting unit of porphyrinoid-CD conjugates, under the PCI protocol.

Experimental section

Materials and Methods

The reagents were of the highest commercial grade available and were used without further purification. Flash column chromatographic purifications were performed using silica gel (pore size 60 Å, 230–400 mesh, Sigma-Aldrich) and thin-layer chromatography was performed on silica gel 60 F254 plates. Benzoylated cellulose tubing (MWCO = 2000) from Sigma was used for dialysis. Cell experiments: the media/agents, LysoTracker® Green DND-26 and Nunc™ glass base dishes for the cultures of cells were purchased from Thermo Fisher Scientific. 3-(4,5-Dimethylthiazol-2-yl)-2,5-diphenyl-2H-tetrazolium bromide (MTT) was a product of Sigma-Aldrich. Instrumentation and methods for structural, photophysical and nanoparticle characterization are briefly described in the Supplementary materials section. A home-made cylindrical photoreactor with SMD 5050 LED tape (viewing angle of elements 120°) set at 630 ± 10 nm and 0.741 W (3.94 ± 0.12 mW/cm^2) and a power supply fixed at 12 V was used for photostability and $^1O_2$ production tests. Another home-made LED array lamp comprising 56×5 mm LEDs emitting at 640 ± 13 nm, viewing angle 20° (Kingbright Electronic CO, LTD) and a power supply adjusted at 20 V with 6.97 ± 0.14 mW/cm^2 LED output, was used for the irradiation of 96-well plates. The lamp was secured at 2 cm over each plate (1 LED/well). Extensive experimental details on all methods have been published previously.[19b,7]

Biological Experiments

Cell culture. MCF-7 human breast adenocarcinoma cell lines were grown as reported.[19b,7] The stock solutions of the chlorin-βCD conjugates or mTHPC (100 μM) or the corresponding complexes with TamCit[7] (75 μM) in PBS with 4% DMSO (v/v), respectively, after 2 min of sonication and 2 h stirring were diluted with culture media and were allowed to self-assemble for 24 h. Final concentrations [Conjugates]:[TamCit] = 10 μM:7.5 μM.

Confocal Microscopy. MCF-7 cells were seeded on glass base dishes (1×10^5 cells per dish) and allowed to grow overnight in DMEM complete media (2 mL), in the same conditions as for the cell culture. The cells were subsequently treated with solutions of chlorin-βCD conjugates or with mTHPC. These solutions, prepared with 2 min of sonication followed by 2 h stirring, were added to the culture medium and the cells were incubated for 24 h (10 μM final concentration). The samples were examined on a Leica TCS SP8 MP (Wetzlar, Germany) multiphoton confocal microscope, described previously.[19b,7] After the 24 h incubation of cells, LysoTracker® Green DND-26 was added to a final concentration of 10 nm (stock solution 1 mM in DMSO) for approx. 5 min. The samples were excited at 514 nm (1.3% laser intensity), and emission was recorded between 637 and 670 nm, while LysoTracker® Green DND-26 was excited at 488 nm (0.2% laser intensity) and emission was recorded between 501 and 538 nm. LAS X software was used to acquire images. Processing was carried out with Image J.

Dark toxicity assays.[19b,7] The *in vitro* MCF-7 cell dark cytotoxicity assays in the presence of the compounds alone or loaded with TamCit were conducted using the MTT colorimetric assay. The cells were seeded in 96-well plates (1×10^4 cells/well in 100 μL culture medium) and left to incubate for 24 h in complete medium with 10% FBS at 37 °C in a 5% CO_2 incubator. The cells were subsequently incubated for 24 h with the pre-assembled conjugates (10 μM, DMSO content 0.4%, v/v). Pre-assembly was performed using 100 μM stock solutions in PBS with 4% v/v DMSO which were sonicated for 2 min, stirred for 2 h, then diluted 10-fold with the culture medium and allowed to stand for 24 h. The assay was performed as reported before.[19b,7] The results were expressed as % cell viability = (mean optical density (OD) of treated cells/mean OD of untreated cells)×100 *vs.* concentration. All measurements were carried out in quadruplicates and data were expressed as mean ± standard deviation.

Phototoxicity assays. Cells were seeded (1×10^4 or 3×10^3 cells/well in 100 μL culture medium) into 96-well plates and left to incubate for 24 h in complete media. The stock solutions of either free conjugates (100 μM) or conjugates (100 μM) + TamCit (75 μM) were sonicated for 2 min, stirred for 2 h, added to the culture medium and incubated for 24 h to assemble. Final concentrations: 10 μM conjugate, and 10 μM conjugate with 7.5 μM TamCit, final DMSO content 0.4%, v/v. After 24 h incubation with the assemblies the cells were washed with PBS and fresh complete medium was added. The cells were irradiated immediately at 640 nm at different time points. After the irradiation, the cells were incubated for additional 24 or 48 h, then washed with PBS, fresh medium was added and viability was assessed with the MTT assay. Control values were measured with untreated cells with and without irradiation. All measurements were carried out in quadruplicates and data were expressed as mean ± standard deviation.

Synthesis

Tamoxifen citrate (TamCit, tamoxifen:citrate = 2:1) and TPPOCNHbmC5 (MALDI-TOF HRMS for $C_{91}H_{107}N_5O_{36}$: calcd: 1845.6696; found: 1845.6680, $[M]^+$) were synthesized as reported.[7] 5,10,15,20-Tetra(3-hydroxyphenyl)-porphyrin (mTHPP) was prepared as reported.[19b] 5–10,15,20-Tetra(3-hydroxyphenyl)chlorin (mTHPC, MALDI-TOF HRMS for C44H32 N4O4: calcd: 680.240; found 681.037 $[M+H]^+$, α-cyano-4-hydroxycinnamicc acid (HCCA) matrix) was prepared from mTHPP as reported:[9] ^{1}H NMR (500 MHz, 298.0 K,

DMSO-d_6): δ 9.76 (OH, br s, ~4H), 8.62 ($Pyr_{1,3}$, d, J=4.5 Hz, 2H), 8.36 (Pyr_2, s, 2H), 8.23 ($Pyr_{1,3}$, d, J=4.5 Hz, 2H), 7.62–7.09 (Ph, *o′,o,m,p*, m, 16H), 4.15 (HPyr, s, 4H), −1.66 (NH, s, 2H) ppm, in accordance with the literature.[9] The product did not contain unreacted porphyrin. mTHPPCD was synthesized as described[6] and was identical with an authentic sample.[6]

mTHPCCD: The porphyrin-β-cyclodextrin conjugate mTHPPCD (20 mg, 0.011 mmol) was dissolved in dry pyridine (0.6 mL) under Ar, while protected from light. To this solution, K_2CO_3 (6.2 mg, 0.044 mmol) and *p*-toluenesulfonyl hydrazide (8.3 mg, 0.044 mmol) were added and the mixture was heated under reflux. Additional K_2CO_3 (6.2 mg, 0.044 mmol) and *p*-toluenesulfonyl hydrazide (8.3 mg, 0.044 mmol) were added in 4 portions and stirring was continued under reflux for 48 h. Analysis of the visible spectrum of the crude product showed that it was a mixture of the desired chlorin and the corresponding bacteriochlorin (UV-Vis absorption bands at 650 and 740 nm, respectively). Thus, the mixture was allowed to stir in the air at 120 °C for 15 min, until the entire amount of pyridine was evaporated. Subsequently, 1.5 mL of H_2O was added and the mixture was stirred vigorously at 0 °C. The solution was neutralized carefully with HCl (37% w/w), the solid was dialyzed for 48 h, and the product was collected as a brown solid (mixture of chlorins and bacteriochlorin) after solvent evaporation. This solid was dissolved in DMF (20 mL) and tetrachloro-*o*-benzoquinone (*o*-chloranil, 2.2 mg, 0.009 mmol) was added while stirring at 25 °C. The progress of the reaction was continuously monitored by UV-Vis spectroscopy. As soon as the peak of bacteriochlorin (740 nm) completely disappeared, the reaction mixture was quenched with triethylamine followed by evaporation of the solvent. The pH was adjusted to ~6 to 7 and the product was dialyzed for 18 h. Solvent removal afforded the mTHPCCD conjugate as a black crystalline solid (19 mg, 95%). The content of unreacted porphyrin was <4%. ^{1}H NMR (500 MHz, 298.1 K, DMSO-d_6): δ 9.80 (Ph-OH, br s, 3 h), 8.63 ($Pyr_{1,3}$, m, 2H), 8.36 (Pyr_2, m, 2H), 8.23 ($Pyr_{1,3}$, m, 2H), 7.5 (*m*, m, 4H), 7.39 (*o,o′*, m, 8H), 7.14 (*p*, m, 4H), 6.00–5.20 (CD-OH, m, 14H), 4.86 (CD–H1, m, 7H), 4.38 (CD-CH_2-OH, m, 6H), 4.16 ($HPyr_4$, m, 4H), 3.57 (CD–H6,3,2, m, 28H), 3.30 (CD–H4,5, m, 14H), −1.64, −1.66 (NH isomer 1 and isomer 2, two br s, 2H) ppm. MALDI-TOF HRMS for $C_{86}H_{100}N_4O_{38}$: calcd: 1796.6016; found: *m/e* 1796.6023 (M^+, isomer 1 and isomer 2).

TPCOCNHbmC5: The compound was synthesized from TPPOCNHbmC5 (21 mg, 0.011 mmol) following the procedure described above, without the tetrachloro-*o*-benzoquinone reaction step, due to the fact that after work-up the absorption peak of bacteriochlorin (740 nm) had completely disappeared. TPCOCNHbmC5 was collected as a black crystalline solid (15 mg, 72%). The content of unreacted porphyrin was <10%. ^{1}H NMR (500 MHz, 298.1 K, DMSO-d_6): δ 8.60 ($Pyr_{1,3}$, m, 2H), 8.29 (Pyr_2, m, 2H), 8.16 ($Pyr_{1,3}$, m, 2H), 8.07–6.86 (Ph *o,o′,p,m,m′*, m, 16H), 5.73 (CD-OH, m, 14H), 4.83 (CD–H1, m, 7H), 4.45 (CD-CH_2-OH, m, 6H), 4.05 ($HPyr_4$, m, 4H), 3.64 (CD–H3,6,5,6′, m, 27H), 3.33 (CD–H4,2,6′, m, 15H), 2.18 (H4′, m, 2H), 1.69 (H2′,3′, m, 4H), −1.54, −1.59 (NH isomer 1 and isomer 2, two br s, 2H) ppm. MALDI-TOF HRMS for $C_{91}H_{109}N_5O_{36}$: calcd: 1847.6852; found: *m/e* 1848.6938 ($[M+H]^+$, isomer 1 and isomer 2).

Supporting Information

General description of instrumentation and supplementary Figures and Tables for structural and spectroscopic characterization, 2D NMR data, DLS diagrams and irradiation tests are shown. The authors have cited an additional reference within the Supporting Information.[27]

Acknowledgements

Funding by the General Secretariat for Research and Technology (Greece) for the project PCInano (T3EPA-0048) in the frame of EuroNanoMed-II is gratefully acknowledged. Fruitful discussions with Prof. K. Berg and Dr. T.A. Theodossiou, Oslo University Hospital, Norway, and support for open access publication by HEAL-Link are also gratefully acknowledged.

Conflict of Interests

The authors declare no conflict of interest.

Data Availability Statement

The data that support the findings of this study are available in the supplementary material of this article.

Keywords: Aggregation · chlorin · conjugates · cyclodextrins · drug delivery · PCI

[1] T. Loftsson, P. Jarho, M. Másson, T. Järvinen, *Expert Opin. Drug Delivery* **2005**, *2*, 335–251.
[2] R. M. Haley, R. Gottardi, R. Langer, M. J. Mitchell, *Drug Delivery Transl. Res.* **2020**, *10*, 661–677.
[3] a) D. E. J. G. J. Dolmans, D. Fukumura, R. K. Jain, *Nat. Rev. Cancer* **2003**, *3*, 380–387; b) A. E. O'Connor, W. M. Gallagher, A. T. Byrne, *Photochem. Photobiol.* **2009**, *85*, 1053–1074; c) A. P. Castano, P. Mroz, M. R. Hamblin, *Nat. Rev. Cancer* **2006**, *6*, 535–545.
[4] a) K. Berg, P. K. Selbo, L. Prasmickaite, T. E. Tjelle, K. Sandvig, J. Moan, G. Gaudernack, O. Fodstad, S. Kjølsrud, H. Anholt, G. H. Rodal, S. K. Rodal, A. Høgset, *Cancer Res.* **1999**, *59*,1180–1183; b) K. Berg, A. Weyergang, L. Prasmickaite, A. Bonsted, A. Høgset, M.-T. R. Strand, E. Wagner, P. K. Selbo, *Methods Mol. Biol.* **2010** *635*, 133–145; c) H. Hirschberg, K. Berg, Q. Peng, *Neuroimmunol. Neuroinflammation* **2018**, *5*, 27.
[5] I. M. Mavridis, K. Yannakopoulou, *J. Med. Chem.* **2020**, 3391–3424 and references cited therein.
[6] T. A. Theodossiou, A. R. Goncalves, K. Yannakopoulou, E. Skarpen, K. Berg, *Angew. Chem. Int. Ed.* **2015**, *54*, 4885–4889.
[7] S. Panagiotakis, B. Mavroidi, A. Athanasopoulos, A. R. Gonçalves, L. Bugnicourt-Moreira, T. Regagnon, N. Boukos, G. Charalambidis, A. G. Coutsolelos, M. Grigalavicius, T. A. Theodossiou, K. Berg, C. Ladavière, M. Pelecanou, K. Yannakopoulou, *Carbohydr. Polym.* **2023**, *306*, 120579.
[8] R. Baskaran, J. Lee, S.-G. Yang, *Biomaterials Res.* **2018**, *22*, 25.
[9] R. Bonnett, R. D. White, U.-J. Winfield, M. C. Berenbaum, *Biochem. J.* **1989**, *261*, 277–280.
[10] a) L. Ma, J. Moan, K. Berg, *Int. J. Cancer* **1994**, *57*, 883–888; b) A. Wiehe, M. O. Senge, *Photochem. Photobiol.* **2023**, *99*, 356–419.
[11] J. Nuno Silva, A. M. G. Silva, J. P. Tomé, A. O. Ribeiro, M. R. M. Domingues, J. A. S. Cavaleiro, A. M. S. Silva, M. Graça, P. M. S. Neves, A. C. Tomé, O. A. Serra, F. Bosca, P. Filipe, R. Santuse, P. Morlière, *Photochem. Photobiol. Sci.* **2008**, *7*, 834–843.
[12] H. Kim, M. W. Kim, Y.-IL Jeong, H. S. Yang, *Cells* **2021**, *10*, 2190.
[13] a) H. W. Whitlock Jr., R. Hanauer, Y. Oester, B. K. Bower, *J. Am. Chem. Soc.* **1969**, *91*, 7485–7489; b) M. Taniguchi, J. S. Lindsay, *Chem. Rev.* **2017**, *1127*, 344–535.
[14] I. Laville, T. Figueiredo, B. Loock, S. Pigaglio, Ph. Maillard, D. S. Grierson, D. Carrez, A. Croisy, J. Blais, *Bioorg. Med. Chem.* **2003**, *11*, 1643–1652.

[15] J. Helaja, M. Stapelbroek-Möllmann, I. Kilpeläinen, P. H. Hynninen, *J. Org. Chem.* **2000**, *65*, 3700–3707.
[16] V. Sambhaji Gaware, M. Hakerud, A. Juzeniene, A. Høgset, K. Berg, M. Másson, *Biomacromolecules* **2017**, *18*, 1108–1126.
[17] A. Bautista-Sanchez, A. Kasselouri, M.-C. Desroches, J. Blais, P. Maillard, D. Manfrim de Oliveira, A. C. Tedesco, P. Prognon, J. Delaire, *J. Photochem. Photobiol. B* **2005**, *81*, 154–162.
[18] a) I. Belitchenko, V. Melnikova, L. Bezdetnaya, H. Rezzoug, J. L. Merlin, A. Potapenko, F. Guillemin, *Photochem. Photobiol.* **1998**, *67*, 584–590; b) N. C. Maiti, S. Mazumdar, N. Periasamy, *J. Phys. Chem. B* **1998**, *102*, 1528–1538; c) A. R. Antonangelo, K. C. M. Westrup, L. A. Burt, C. Grazia Bezzu, T. Malewschik, G. S. Machado, F. S. Nunes, N. B. McKeown, S. Nakagaki, *RSC Adv.* **2017**, *7*, 50610–50618; d) F. Bächle, C. Maichle-Mössmer, T. Ziegler, *ChemPlusChem* **2019**, *84*, 1081–1093; e) K. Cai, J. Xie, D. Zhang, W. Shi, Q. Yan, D. Zhao, *J. Am. Chem. Soc.* **2018**, *140*, 5764–5773.
[19] a) H. Kitagishi, F. Chai, S. Negi, Y. Sugiura, K. Kano, *Chem. Commun.* **2015**, *51*, 2421–2424; b) S. Panagiotakis, B. Mavroidi, A. Athanasopoulos, G. Charalambidis, A. G. Coutsolelos, M. Paravatou-Petsotas, M. Pelecanou, I. M. Mavridis, K. Yannakopoulou, *Carbohydr. Polym.* **2022**, *75*, 118666.
[20] I. Yakavets, I. Yankovsky, M. Millard, L. Lamy, H.-P. Lassalle, A. Wiehed, V. Zorin, L. Bezdetnaya, *Int. J. Pharm.* **2017**, *529*, 568–575.
[21] Y. Shi, F. Zhang, R. F. J. Linhardt, *Dyes Pigm.* **2021**, *188*, 109136.
[22] V. Kirejev, A. R. Gonçalves, C. Aggelidou, I. Manet, J. Mårtensson, K. Yannakopoulou, M. B. Ericson, *Photochem. Photobiol. Sci.* **2014**, *13*, 1185–1191.
[23] C. Aggelidou, T. A. Theodossiou, K. Yannakopoulou, *Photochem. Photobiol.* **2013**, *89*, 1011–1019.
[24] M. Messner, S. V. Kurkov, Ph. Jansook, Th. Loftsson, *Int. J. Pharm.* **2010**, *387*, 199–208.
[25] S. Marchal, A. François, D. Dumas, F. Guillemin, L. Bezdetnaya, *Br. J. Cancer* **2007**, *96*, 944–951.
[26] R. Song, Y. Feng, D. Wang, Z. Xu, Z. Li, X. Shao, *Sci. Rep.* **2017**, *7*, 42058.
[27] A. P. Thordarson, *Chem. Soc. Rev.* **2011**, *40*, 1305–1323.

Manuscript received: December 15, 2023
Revised manuscript received: February 2, 2024
Accepted manuscript online: February 12, 2024
Version of record online: February 29, 2024